Macromolecular Materials and Engineering
www.mme-journal.de

Enhancement of Mechanical Properties of FDM-PLA Parts via Thermal Annealing

Radoslaw A. Wach, Piotr Wolszczak, and Agnieszka Adamus-Wlodarczyk*

The objective of this study is to investigate the possibility of enhancing mechanical properties of poly(lactic acid) (PLA) samples processed by a rapid manufacturing (RM) technique by increasing PLA crystallinity degree via thermal annealing. The samples are manufactured by fused deposition modeling (FDM) at different temperatures and subsequently evaluated by three-point bending flexural and tensile tests. The polymer processed at 215 °C is thermally annealed over its glass transition temperature in order to increase the degree of crystallinity to the maximum attainable level as measured by the differential scanning calorimetry and confirmed by X-ray diffraction. The increase in the degree of crystallinity of FDM-PLA enhances flexural stress of the samples by 11–17%. The study also demonstrates applicability of radiation sterilization for FDM-PLA parts. Therefore, thermal annealing might be introduced into a standard RM technology of PLA, particularly for sterilizable customized implants, to efficiently improve their mechanical properties.

1. Introduction

Fused deposition modeling (FDM) is a versatile and innovative way of manufacturing objects of any shape and geometry, especially objects with complex design features that are infeasible to create by other methods. This technique is also perfectly suited for prototyping, 3D visualization of projects, and fabrication of short series of objects and parts. One of its interesting applications is the possibility of printing customized implants from biodegradable materials. Although the printing of cells combined with organic matter for the construction of hybrid organs still requires years of investigation,[1] the problem of constructing matrices for cell seeding for tissue engineering or microfluidic devices has been studied thoroughly.[2,3] Despite its unquestionable advantages, FDM of molten polymers still poses some challenges with respect to surface quality and the quality of fusion of adjacent layers that affect the functional properties of printed parts. Therefore, it is necessary to assess bulk properties of the processed material and its structural features resulting from printing in order to elaborate processing and post-treatment methods and optimize their conditions.[4–6]

Polyesters, like poly(lactic acid) (PLA), are popular biodegradable thermoplastics processed by typical thermal and solvent methods, such as injection moulding, extrusion, spinning, casting, etc.[6,7] In the biomedical field, semicrystalline PLA polymer is an appropriate material for load bearing applications,[8,9] also when blended with other polyesters to improve mechanical properties of the material.[10] Customized biodegradable implants can be manufactured from PLA by rapid manufacturing (RM) techniques, including FDM or 3D printing.[11–13] Nevertheless, when designing a shape to be manufactured by FDM technique that will satisfy certain (bio)mechanical parameters, for example, strength, one should optimize processing parameters for the particular PLA material, such as strand diameter or layer height, infill density, printing temperature, cooling rate, build platform temperature, etc.[14,15]

Mechanical properties of biodegradable synthetic polymers and, in general, semicrystalline thermoplastics are a function of the degree of crystallinity (χ) of the polymer.[16] The crystallization of a thermoplastic polymer is related to its microstructure and—unlike in the case of metal melts—restricted by the mobility of chain segments. Limitation of the chain segments' mobility results from inherent viscosity of the material, which is a function of polymer microstructure, molecular weight, and temperature.[17,18] The arrangement of molecular chain segments into ordered structures during thermal processing is arrested at high cooling rates, completely stopping below the glass transition temperature (T_g). The supercooled state can be attained if the sample is instantly cooled from melt to below T_g; then, in principle, no crystalline phase is formed. This might be the case with FDM, when the molten polymer extruded through the heated nozzle of the printer fuses with the material in the preceding layer and immediately cools down. At this nonequilibrium transition, a metastable phase is formed, yet the crystallization potential of the material is not exhausted. Moreover, variation in the thermal characteristics occurs between different strands, though the degree of crystallinity of the polymer at the top and side strands is usually lower due to faster cooling and that of the bottom layers is determined by the build platform temperature, that is, higher temperature favors obtaining

Dr. R. A. Wach, Dr. A. Adamus-Wlodarczyk
Institute of Applied Radiation Chemistry
Faculty of Chemistry, Lodz University of Technology
Wroblewskiego 15, 93-590 Lodz, Poland
E-mail: wach@mitr.p.lodz.pl
Dr. P. Wolszczak
Department of Automation
Lublin University of Technology
Nadbystrzycka 38D, 20-618 Lublin, Poland
The ORCID identification number(s) for the author(s) of this article can be found under https://doi.org/10.1002/mame.201800169.

DOI: 10.1002/mame.201800169

higher crystallinity.[19,20] In order to complete the crystallization of PLA, either in pure form or constituting the matrix of a composite, that is, to increase the crystallinity degree of the material processed by various thermal and solvent methods, a subsequent annealing treatment may be required.[21–23]

This, in turn, would enhance mechanical properties of the resulting material.[24] During thermal conditioning, at a temperature over T_g, polymeric macromolecules gain in mobility, which allows for the rearrangement of segments and the formation of an ordered phase. Usually, material of higher strength can be obtained after annealing, but it is necessary to note that particular thermal conditions, for example, cooling of samples after melting at a temperature slightly above the T_g that causes high level of chain packaging, may result in a ductile polymer; this shear yielding can be advantageous for certain applications.[25]

The objective of this study was to investigate the supercooling phenomenon in FDM-PLA using a commercial printing system, and to optimize the temperature and time of thermal annealing of manufactured parts to achieve the maximal degree of crystallinity. The impact of the degree of crystallinity and the use of electron beam irradiation as the sterilization method on mechanical properties of FDM-PLA parts is investigated as well.

2. Experimental Section

2.1. Materials

Commercial poly(lactic acid) filament of 1.75 mm diameter (Finnotech Co., Poland) was used for the processing of test samples by FDM. Number-average (M_n) and weight-average (M_w) molecular weights of PLA in the original thread of 60 and 120 kg mol^{-1} were determined by GPC. Based on polarimetry measurements in a methylene chloride solvent conducted on the polymer after the removal of a dye with active carbon, the D-lactide content was determined to be 14%.

2.2. FDM of PLA

The Idea Lab One FDM instrument (Idea Lab Co., Poland) was used to manufacture test samples. The machine was equipped with a 0.5 mm diameter nozzle with a heater, cooling fan, and heated build platform (up to 120 °C) movable in three directions. The working space was confined to a chamber under partly controlled conditions, thereby isolating the working space from air circulation in the experimental room.

The design of two types of test samples (described in Figure S1, Supporting Information) was accomplished with the 3D CAD system SolidEdge, and then used for print path design with Cura and Repetier-Host CAM software. Dumbbells for tensile tests and beams for the three-point bending flexural test conforming to respective ISO standards were manufactured.[26,27] The samples were designed such that the lines of thermally plasticized material were consecutively arranged unidirectionally along the longer dimension of the test sample. The samples were manufactured from the PLA filament on the build platform maintained at 55 °C at the printing temperatures (nozzle temperatures) T_p ranging 195–255 °C. Printing speed of 45 mm s^{-1} at the nozzle position over the preceding layer distance of 0.3 mm resulted in layers of approx. 0.3 mm thick. According to the design, the infill density was 100%—solid shapes were anticipated. Nevertheless, regular voids were detected at a cross-section of the samples upon visual examination. The size and frequency of the voids depend on the nozzle temperature and sample height. The voids were detected especially in the upper region of the samples manufactured at a lower T_p, up to 200 °C. Sample bottom layers attached to the build platform were inherently solid without any voids between the consecutive lines (see Figure S2, Supporting Information). The increase in the nozzle temperature reduced the occurrence of voids, therefore the samples produced at higher temperatures were considered for testing. The T_p selected, after the initial assessment (see Section 3.1.), for further experiments was 215 °C, and the samples produced at this temperature were characterized by high infill density, the voids comprise 3.50% (SD 1.16%). The void percentage did not change after thermal annealing, within experimental error. The manufactured samples were subjected to thermal annealing in a DSC furnace during heating scan and, alternatively, in a laboratory drier with natural air circulation in the temperature range 65–95 °C.

2.3. Viscometry, GPC

In order to determine viscosity-average molecular weight, intrinsic viscosities of PLA samples were measured in chloroform at 25.0 °C with the AVS-310 automatic viscometry system (Schott Geräte) equipped with the 01/0a type Ubbelohde capillary. Samples with an initial concentration of 10 g L^{-1} were filtered through 0.45 µm PTFE membrane filters (Sartorius) prior to the analysis. Gel permeation chromatography (GPC) measurements were conducted using a system equipped with the P580 pump (Dionex), two columns of 10 µm and 5 µm pore size (Knauer), and three detectors: Viscotec Ralls Detector (static light scattering at 90° at a wavelength of 670 nm) and Viscotec Dual Detector 250 (refractometer/viscometer). Dichloromethane was used as an eluent at 30 °C with a flow rate of 0.8 mL min^{-1}. Sample concentrations in the range 8–10 g L^{-1} and injection volumes of 100 mL were applied. All solutions were filtered prior to injection into the GPC column through 0.45 µm PTFE membrane filters (Sartorius).

2.4. Thermal Characterization

The thermal analysis was carried out using the differential scanning calorimetry, DSC Q200 (TA Instruments, USA) in the temperature range 25–200 °C and with a heating rate of 10 °C min^{-1}. Samples for the DSC measurements comprising few inner layers with respect to the height and the width were cut out from the cross-sectional part of the specimen. Two replications were done for the evaluation of thermal properties for the experiment of printing temperature selection and at least three measurements were conducted for all other experiments; average values are presented.

Changes in the glass transition temperature (T_g) and melting temperature (T_m) were determined. The degree of

crystallinity (χ) was determined from a thermal effect accompanying melting or crystallization via the following formula:

$$\chi = \frac{\Delta H}{\Delta H_0} \quad (1)$$

where ΔH is the enthalpy of fusion of test sample, ΔH_0 denotes the enthalpy of fusion of a 100% crystalline sample. If the cold crystallization and exothermic reordering emerged, their enthalpies was subtracted from the ΔH to calculate the χ of the sample before the measurement, thus to determine the degree of crystallinity of the initial and thermally annealed PLA specimens. The crystalline fractions were calculated assuming the fusion enthalpy value ΔH_0 of 93.64 J g^{-1} for 100% crystalline PLA.[28]

2.5. X-Ray Diffraction (XRD)

The phase composition in FDM-PLA samples was measured by the X-ray diffraction technique using the Empyrean diffractometer (Panalytical) with Cu Ka radiation (0.1542515 nm) working in the grazing incidence XRD (GIXRD) mode. The incident beam angle was set to 3°. Data processing was done with the High Score Plus software.

The size of crystallites was determined based on X-ray diffraction peaks and the Scherrer formula:

$$B(2\theta) = \frac{0.94\lambda}{L\cos\theta} \quad (2)$$

where B is the full width of the peak, 2θ is the scattering angle in radians, λ is the wavelength, 0.94 is a constant depending on the function used to fit the peak, and L is the diameter of the crystallites.[29]

2.6. Mechanical Testing

The three-point bending tests were conducted using the Zwick Roell Z2 testing machine (Germany) in accordance with EN ISO 178:2011. Eighty-eight millimeter bars with 10 mm width and 4 mm height were placed on two supporting pins with a 56 mm span. The load was applied at the center of the sample with a 2 kN head moving at the speed of 5 mm min^{-1} (Figure S3a, Supporting Information). Tensile testing was conducted with the QC-Tech B-1 according to EN ISO 527-2:2012. The standardized dumbbells with a 160 mm length, narrowed at the distance of 80 mm, were placed in clamps attached to the head moving at the speed of 1 mm min^{-1} (Figure S3b, Supporting Information). At least five samples for each data-point were tested.

2.7. Sterilization

The effect of sterilization on the inherent and mechanical properties of the FDM-PLA material was determined via the radiation sterilization method. Vacuum-packed samples were irradiated with a dose of 25 kGy (in some cases, 50 kGy) of the electron beam (EB) generated with the ELU-6 accelerator of 6 MeV.

3. Results and Discussion

3.1. Influence of Printing Temperature on Mechanical Parameters of FDM-PLA Parts

The FDM processing is characterized by the anisotropy of longer samples prepared for mechanical tests. The longer dimension was preferred since the samples were printed in a horizontal direction, with a low height-to-width ratio, resulting in the lowest possible number of printed layers and therefore the lowest number of fusion interfaces. Consequently, samples with the best performance in terms of testing direction were produced. Additionally, the designed path trajectories ensured stable conditions for the flow of the material from the nozzle (hot-end). All potential defects in the laying direction occurred outside the zone subjected to mechanical testing.

Initial experiments were designed to select the potentially most suitable T_p for producing a material with good mechanical properties. The nozzle temperature range 195–255 °C was applied to manufactured samples for three-point flexural and tensile tests, the results of which are reported in **Figures 1** and **2**, respectively. The samples produced at 200 °C and lower exhibit significantly lower flexural stress and modulus—they

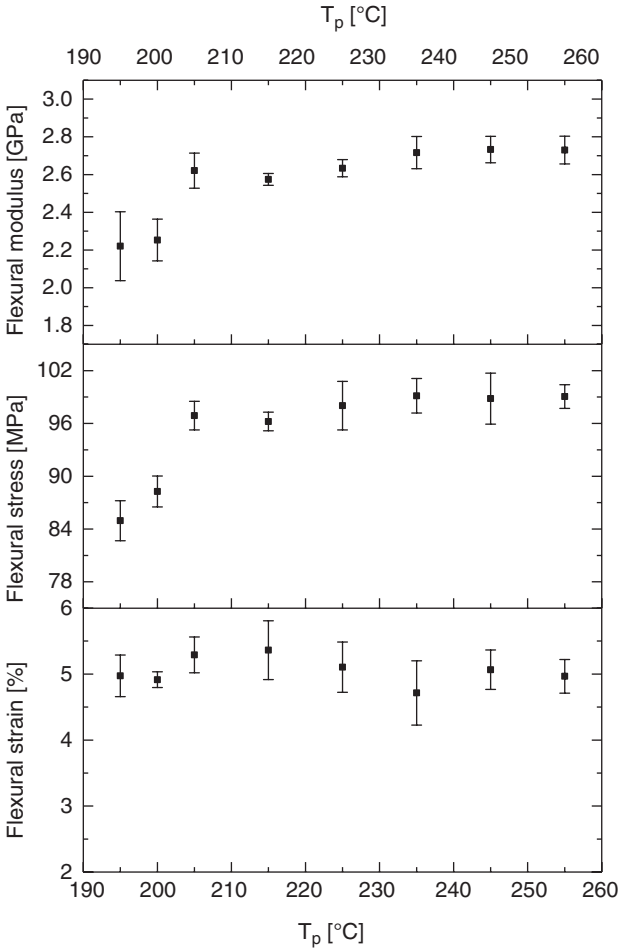

Figure 1. Change of flexural parameters of FDM-PLA bars at various nozzle temperatures T_p as measured in the three-point bending flexural test.

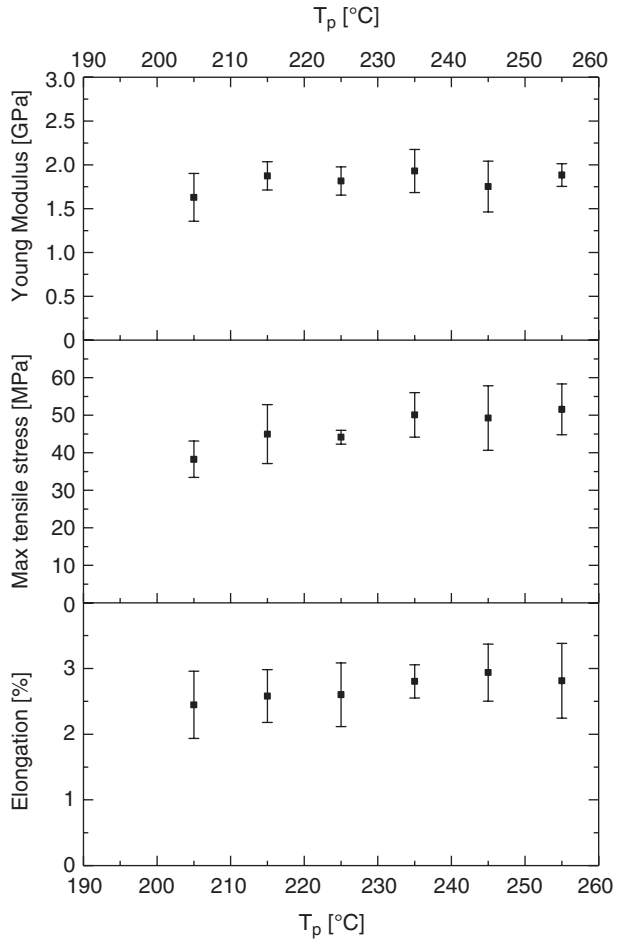

Figure 2. Change of mechanical parameters of FDM-PLA dumbbells at various nozzle temperatures T_p as measured in the tensile test.

are by approx. 20% lower than those measured in the samples printed at higher nozzle temperatures. The flexural parameters of the PLA material are the same irrespective of the printing temperature if processed at 205 °C and higher—the flexural stress is approx. 95 MPa and the flexural modulus is over 2.6 GPa. The flexural strain at the maximum stress is approx. 5.5%. Since the material processed at the temperature below 205 °C revealed unsatisfactory performance in the bending test, tensile measurements were conducted for the samples produced at the temperature not lower than 205 °C. The maximum tensile stress and Young modulus range approx. 40 to over 50 MPa and 1.6–2.0 GPa, respectively. The values of tensile parameters slightly increase with increasing the printing temperature. The strain at maximum tensile stress is about 2.5% and does not depend on T_p. The mechanical parameters of the FDM-PLA samples are within the characteristic range for the PLA processed via conventional methods.[30]

The thermal characteristics, that is, heat flow measured by DSC, and determined values of thermal properties of the samples manufactured at various nozzle temperatures are presented in Figure S4 and Table S1, Supporting Information, respectively. The profiles of PLA heat flow during the first heating, cooling, and the second heating are typical of this thermoplastic.[31] The glass transition temperature T_g determined from the second heating scan ranges 62.4 ± 0.12 °C while the peak-melting of the crystalline phase during the first heating occurs at T_m ranging 153.4 ± 0.75 °C and is at about 2.6 °C higher at the second heating. Every sample reveals cold crystallization at T_c ranging 116.6 ± 0.71 °C. The presence of cold crystallization reflects the thermal history of the material. In the present case, the thermal effect of cold crystallization ΔH_{cI} ranges 19.7 ± 2.11 J g^{-1}, whereas the heat of melting ΔH_{mI} equals 23.3 ± 1.27 J g^{-1}; therefore, the enthalpy of fusion resulting from their difference reflects the degree of crystallinity of the samples after printing, χ_0, determined by Equation (1) ranges 3.6 ± 1.90%. The intrinsic degree of crystallinity of the untreated PLA material, as determined from the endothermal peak of melting ΔH_m (first and second heating), was calculated to be 23–25%. The relatively low crystallinity degree and low T_m result from two isomeric forms of PLA, the major L-isomer constitutes 86% of the material.[32] The PLA samples were maintained at ambient temperature during FDM processing, and the cooling of every line, after fusion with the bottom and adjacent lines, was rapid. The temperature reduction to below T_g occurred at approx. 20 s, as reported previously.[6] Thus, the majority of the material preserved the amorphous phase—the polymer chains were unable to form an ordered structure to reduce the entropy of the system due to a lack of sufficient activation energy—therefore, this supercooled state poses an intrinsic potential for further crystallization.

Given the low crystallinity degree of the PLA material after processing, it was expected that its increase might positively affect the mechanical performance of printed parts. Since the lowest temperature of 215 °C yielded samples with good mechanical performance, this temperature value was selected for manufacturing samples for further tests. It is a well-known fact that PLA degrades upon prolonged annealing at temperatures over 200 °C[33]; therefore, the time and temperature of thermal processing should be maintained as low as possible to ensure appropriate rheology of the thermoplastic melt during extrusion. This approach is also recommended in industrial applications for an economic reason, due to high energy consumption of the thermal manufacturing process.

3.2. Thermal Annealing for Increasing Degree of Crystallinity

The heat distribution and the kinetics of cooling of the PLA material during FDM processing are specific to the particular FDM machine and printing parameters.[6] The PLA material after processing at the applied conditions reached only a partial attainable crystallinity degree, therefore post-processing annealing at elevated temperature, above T_g and below T_m, was employed to increase the degree of crystallinity. Small samples cut out from the FDM-PLA shapes were subjected to thermal treatment in the DSC furnace. The temperature of annealing ranged from slightly above T_g, that is, 65 °C, up to 95 °C. An example of DSC-measured heat flow for the samples maintained at 80 °C for various times is shown in **Figure 3**. The heat flow profile during the first heating is typical of a semicrystalline PLA sample, exhibiting glass transition at T_g, cold crystallization at T_c, and the melting of crystallites at T_m. The distinct

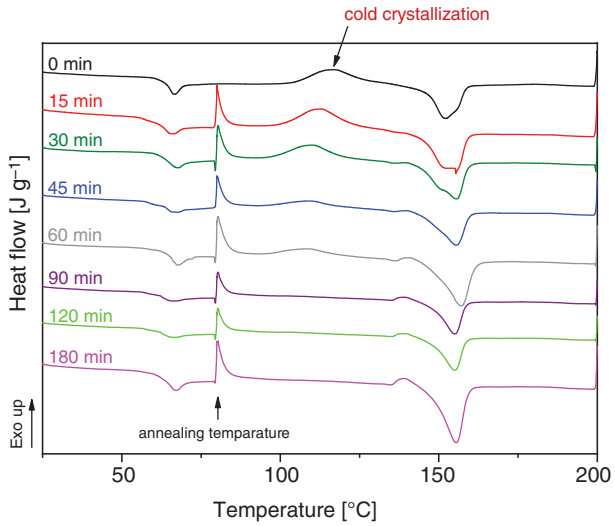

Figure 3. Heat flow during the first heating of PLA samples annealed at 80 °C in DSC furnace for various times (indicated in the graph). Distinct exothermal-like effect is generated by isothermal annealing.

heat transfer signal at 80 °C is caused by annealing when the material forms an ordered phase. This has impact on the cold crystallization exothermal effect, which gradually wears off with increasing time of annealing. The time required for achieving the maximum attainable crystallinity degree at specified annealing temperature is the outcome of these two variables combined, providing information about heat treatment conditions for FDM-PLA parts. In the case in question, the sample had to be kept at 80 °C for 3 h to complete the annealing.

The changes of the cold crystallization exothermal effect in time with respect to annealing temperatures are shown in **Figure 4**. It can be observed that the crystallinity degree of the samples did not increase for the samples kept for 10 h (maximum measurement time) at temperatures slightly exceeding the glass transition temperature for PLA—65 and 70 °C. The ordered phase formation occurs at the temperature of 75 °C and over. Nevertheless, the time required to achieve the maximum χ amounts to a few hours, which may be infeasible in a real technological process. The time was reduced to several tens of minutes with the increase in the annealing temperature and, eventually, less than 10 min was necessary to accomplish the maximum crystallization at 95 °C. Therefore, the two combinations of temperature and time were selected for the annealing of FDM-PLA parts.

3.3. Effect of Annealing on Crystallization

Based on the results of the above-described annealing experiment, the beam-shaped samples were maintained at 85 °C and 95 °C in a regular laboratory drier for 70 and 10 min, respectively. The DSC results of heat transfer measured during the first heating of the annealed samples are shown in **Figure 5**. No exothermal peak of cold crystallization was detected for the samples maintained at 85 °C for 70 min, nevertheless the shorter time of 10 min at the temperature of 95 °C was insufficient to anneal the bulky shape and accomplish the maximum

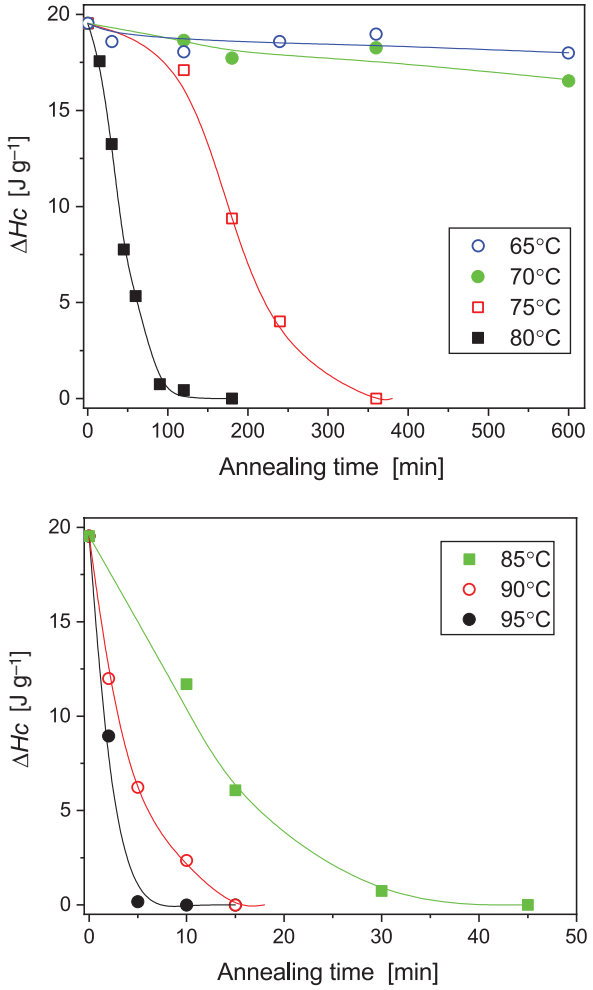

Figure 4. Enthalpy of cold crystallization with respect to time of annealing at various temperatures (indicated in the graphs).

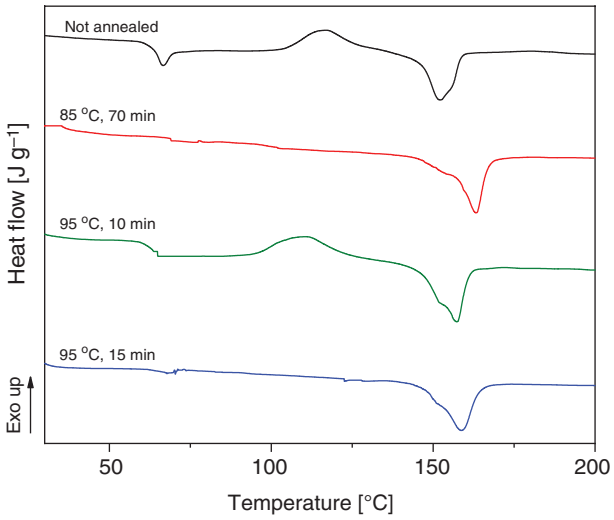

Figure 5. DSC-measured heat flow in the first heating of PLA bars annealed in regular drier. Temperature and time of annealing are indicated in the graph.

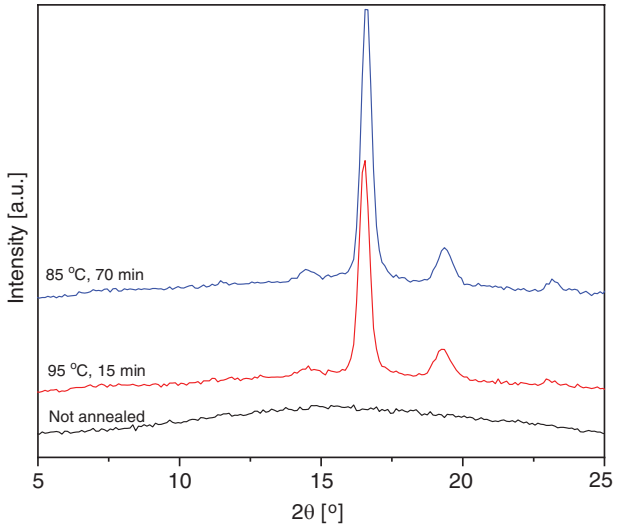

Figure 6. XRD diffraction patterns of PLA bars annealed in regular laboratory drier. Temperature and time of annealing are indicated in the graph.

crystalline fraction. The cold crystallization exothermal heat transfer of 11.0 J g^{-1} with its peak at 110.5 °C was still present. Apparently, the heat transfer to and through the sample was not efficient enough to uniformly anneal the sample. A longer annealing time of 15 min at 95 °C was necessary to complete the process. No cold crystallization was observed, and the resulting χ was over 20%. Other characteristic thermal parameters did not change (see Table S2, Supporting Information).

The PLA samples measured by the DSC method were also examined via XRD, and the obtained diffraction patterns are shown in **Figure 6**. Only the annealed samples, having a significant crystalline part, show diffraction patterns of crystallites, whereas the untreated samples have a wide amorphous halo without crystal peaks. The most pronounced diffraction signal can be observed at 2Θ 16.7; it is accompanied by smaller ones at 2Θ about 14.5, 19.2, and 23.0. The pure P(L-LA)isomer may have two crystal structures: the pseudo-orthorhombic alpha type with the left-handed 10/3 helix of chain conformation-folded crystals, and the orthorhombic beta structure with 3/1 chain conformation-fibrillary crystals.[8] Beta crystallites are less stable and may form at specific conditions, that is, due to hot-drawing at high temperature and high stress. The obtained diffraction patterns correspond to the alpha crystallites of PLA.[23] Therefore, the presence of crystalline fraction of the annealed PLA beams was confirmed with the XRD method, thus supporting the DSC results.

3.4. Effect of Annealing on Mechanical Properties of FDM-PLA Parts

One may expect that increasing the degree of crystallinity would enhance the strength of the PLA material.[34,35] The three-point bending test was employed to assess changes in the flexural properties of the beam samples after annealing. Examples of the stress–strain profiles together with the calculated maximum flexural stresses and flexural strains at maximum stress are

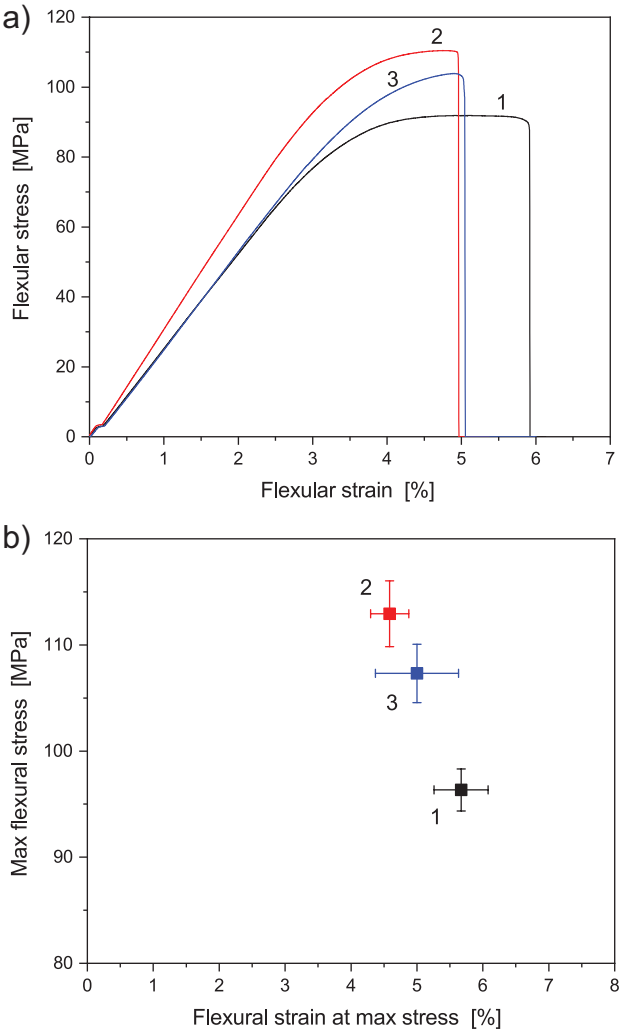

Figure 7. Mechanical properties of untreated FDM samples and samples after thermal annealing in a regular drier oven: 1) untreated sample, 2) sample annealed for 70 min at 85 °C, 3) sample annealed for 15 min at 95 °C. a) Examples of flexural stress–strain profiles, b) maximum flexural stress and flexural strain at maximum stress.

illustrated in **Figure 7**a,b, respectively. The PLA material after thermal annealing at the two applied temperatures exhibits increased crystallinity, which is reflected in its strength. The observed dependency is in line with that reported in the literature demonstrating relation of crystalline fraction and mechanical properties of PLA processed by conventional methods.[34] In the present case, the maximum flexural stress has increased from approx. 96 MPa for the non-annealed samples to approx. 113 and 107 MPa for the samples annealed at 85 °C and 95 °C, which amounts to an increase by 17% and 11%, without any significant change in the flexural strain. Despite the fact that the crystallinity degree for the heat-treated samples is similar (Figures 5 and 6), a slight dependence of the maximum flexural stress on the annealing temperature can be observed (**Table 1**). This might be caused by a somewhat different character of the crystalline phase, since a lower annealing temperature might produce larger crystallites, as can be distinguished from the

Table 1. Flexural properties of FDM-PLA beams after thermal annealing and after sterilization with radiation.

	Flexural stress [MPa]	SD	Bending strain [%]	SD	Flexural modulus [GPa]	SD
Untreated	96.3	2.3	5.67	0.70	2.49	0.22
85 °C, 70 min	112.9	3.1	4.54	0.29	2.71	0.68
95 °C, 15 min	107.3	2.75	4.95	0.63	2.60	0.55
Irradiated 25 kGy	88.7	4.9	4.68	0.14	2.57	0.25
25 kGy and 85 °C, 70 min	74.8	5.4	2.91	0.14	2.69	0.92
95 °C, 15 min and 25 kGy	76.2	5.3	2.51	0.30	3.02	0.23

XRD pattern for those two samples. The crystallites' size calculated from the Scherrer's formula (Equation (2)) were 21.0 and 16.8 nm for FDM-PLA annealing conducted at temperatures 85 °C and 95 °C, respectively. At the higher treatment temperature, there are more nucleation sites and the crystallites grow faster, which results in their smaller size. Larger crystallites, as obtained at lower annealing temperature, results in slightly higher strain and flexural modulus; however, not significantly different than those parameters for samples annealed at 95 °C. Nevertheless, the problem should be investigated further. In spite of the above, the post-processing thermal annealing led to increased mechanical performance of the PLA material.

3.5. Effect of Radiation Sterilization on Mechanical Properties of FDM-PLA Parts

When using PLA as biomaterial for medical devices, it is necessary to determine the effect of selected sterilization method on the properties of the material. Bioburden in and on the device should be reduced practically to zero in order to assure its microbiological safety for the patient. Medical implants made of PLA are typically sterilized by ethylene oxide (EO); however, other low temperature methods such as H_2O_2 cold plasma may also be considered.[36] These methods are perfectly suited for sterilization of bulky solid devices, nevertheless a certain degree of caution should be taken because the sterilizing agent, EO or hydrogen peroxide, is effective only at the surface. What is more, it can affect surface properties, for example, oxidize it. Therefore, biodegradable porous materials or those with voids of specific characteristics should not be sterilized by surface sterilization methods, rather by penetrating techniques. Since thermal methods are not applicable to polymers with low T_g and T_m or to biodegradable polymers, radiation may be the required solution.[37] While the radiation method is used for polymeric biomaterials, one should consider potential changes of properties at either molecular and macroscopic level.

In order to do so, intrinsic viscosity and molecular weight of PLA after radiation sterilization were measured along with flexural properties of the samples. The results of intrinsic viscosity-derived viscosity-average molecular weight, as measured in methylene chloride, and weight-average molecular weight (see Figure S5, Supporting Information for GPC trace) are listed in **Table 2** as a function of radiation sterilization dose. As expected,[38] the molecular weights of PLA decreased by about 1/3 after irradiation with a standard sterilization dose of 25 kGy; with the doubled dose, the reduction was even greater. This can be explained by the occurrence of scission in the main chain resulting from the presence of radiation-vulnerable ester bonds. Besides the crystallinity degree resulting from isomeric purity of the polymer and the thermal history of samples, the molecular weight of PLA is the essential parameter reflecting mechanical properties of the material.

Further, FDM-PLA beams were thermally annealed and irradiated (to simulate radiation sterilization), or first irradiated and then annealed. The flexural properties of the produced samples are listed in Table 1. Since the thermal properties of PLA have positively changed—upsurge of χ to approx. 30% after the irradiation by electron beam with a standard sterilization dose was recorded (**Table 3**, go to Figure S6, Supporting Information for additional explanation)—it is evident that the reduction in molecular weight of the polymer is the key factor negatively affecting the strength of this material. As a result of the application of radiation sterilization, the flexural stress is reduced by approx. 20–30%. The samples become less flexible since an increase in the flexural modulus and significant reduction in the flexural strain can be observed. Therefore, radiation sterilization of the PLA biomaterial can be applied only when the reduced values of strength and elasticity still exceed the acceptable level for a given application, and when stiffness is an important parameter, since it was not changed.

Table 2. Intrinsic viscosity and molecular weight of FDM-PLA after radiation sterilization with EB at 25 and 50 kGy.

Dose [kGy]	Intrinsic viscosity [dm^3 g^{-1}]	Mv[b)] [kg mol^{-1}]	Mw [kg mol^{-1}]
0	1.64[a)]	106.3	120.3
25	1.16	67.8	78.1
50	0.93	50.9	45.7

[a)]Intrinsic viscosity of the PLA in the untreated filament was 1.66 dm^3 g^{-1}; [b)]viscosity average molecular weight was determined from intrinsic viscosity data based on the Mark–Houwink equation assuming constants for PDLLA of k and α equal to $2.21 \cdot 10^{-4}$ g dm^{-3} and 0.77, respectively.[39]

Table 3. Thermal properties of FDM-PLA beams after thermal annealing and after sterilization with radiation.

	T_{gI}	T_{cI}	ΔH_{cI}	T_{mI}	ΔH_{mI}	χ_I	ΔH_{mI}-ΔH_{cI}	χ_a
Untreated	69.1	119.6	18.1	159.0	20.9	22.3	2.8	3.0
85 °C, 70 min	59.9		0	159.3	21.0	22.4	21.0	22.4
95 °C, 15 min	58.5		0	158.1	22.8	24.3	22.8	24.3
Irradiated 25 kGy	64.7	115.4	24.4	160.2	29.0	31.0	29.0	31.0
25 kGy and 85 °C, 70 min	63.8		0	159.4	30.4	32.5	30.4	32.5
95 °C, 15 min and 25 kGy	64.3		0	159.0	30.5	32.6	30.5	32.6

4. Conclusions

The FDM technology enables manufacturing of objects with complex shapes, including those which cannot be created with any other method. The quality and mechanical properties of PLA samples processed with FDM greatly depend on the extrusion temperature. On the one hand, the application of higher temperatures ensures good quality products, due to, for instance, well interconnected interphase between strands. On the other hand, the economic aspects and susceptibility of PLA to thermal degradation recommend the application of lowest possible temperatures to ensure appropriate rheological characteristics of the melt being laid down. To find a compromise between these two viewpoints, in this study the printing temperature was set to 215 °C to produce dumbbell and beam samples for mechanical testing. Crystallinity is a critical factor influencing the strength of a semicrystalline material—this results from intrinsic properties of the polymer and its thermal history, such as the kinetics of cooling in thermal processing. In the employed FDM equipment and processing conditions, the FDM-PLA was characterized by a low degree of crystallinity. Thus, the manufactured samples were thermally treated over the glass transition temperature for PLA in order to increase the fraction of ordered phase. Temperature and time were the controlled variables, that is, a lower annealing temperature required a longer time to achieve the maximum attainable χ, approx. 25%. The thermal treatment of the samples led to an increased strength of the material—the flexural stress increased by approx. 11–17%, whereas no significant change in the modulus was recorded. This may have practical implications. The post-processing annealing may be applied, for instance, to customized PLA implants manufactured with a FDM-processing in order to increase their strength. Nevertheless, changes in the biodegradation kinetics affected by the degree of crystallinity should be taken into account too.

With a great potential for use in biomedical applications, the radiation sterilization method can be applied to PLA only under certain conditions, for example, preferably when the manufactured implant is porous or its surface should not be chemically altered, as often happens with other low temperature sterilization methods. The electron beam as well as gamma rays not only sterilize the surface but also penetrate into internal parts of the material, and despite their reduction, the mechanical properties may still surpass the acceptable level.

The manufacturers of PLA parts by thermal prototyping methods should be aware of the fact that the post-processing treatment affects the operating performance of the FDM material, that is, its mechanical parameters are enhanced due to the increased crystallinity degree caused by the application of thermal annealing.

Supporting Information

Supporting Information is available from the Wiley Online Library or from the author.

Acknowledgements

The authors thank K. Dzierbicka, Eng., for conducting part of the experiments, and Dr. M. Socka of the Polish Academy of Science, Lodz, Poland for characterization of initial PLA.

Conflict of Interest

The authors declare no conflict of interest.

Keywords

crystallinity degree, FDM, poly(lactic acid), radiation sterilization, thermal annealing

Received: March 12, 2018
Revised: May 30, 2018
Published online:

[1] G. Marchioli, L. van Gurp, P. P. van Krieken, D. Stamatialis, M. Engelse, C. A. van Blitterswijk, M. B. J. Karperien, E. de Koning, J. Alblas, L. Moroni, A. A. van Apeldoorn, *Biofabrication* **2015**, *7*, 25009.
[2] R. F. Pereira, P. J. Bártolo, *J. Appl. Polym. Sci.* **2015**, *132*, 42458.
[3] J. Radhakrishnan, A. Subramanian, U. M. Krishnan, S. Sethuraman, *Biomacromolecules* **2017**, *18*, 1.
[4] A. Lanzotti, M. Grasso, G. Staiano, M. Martorelli, *Rapid Prototyp. J.* **2015**, *21*, 604.
[5] J. Torres, M. Cole, A. Owji, Z. DeMastry, A. P. Gordon, *Rapid Prototyp. J.* **2016**, *22*, 387.
[6] P. Wolszczak, K. Łygas, M. Paszko, R. A. Wach, *Rapid Prototyp. J.* **2018**, https://doi.org/10.1108/RPJ-04-2017-0062.
[7] L. T. Lim, R. Auras, M. Rubino, *Prog. Polym. Sci.* **2008**, *33*, 820.
[8] W. Hoogsteen, A. R. Postema, A. J. Pennings, G. T. Brinke, P. Zugenmaier, *Macromolecules* **1990**, *23*, 634.
[9] K. Ong, M. Yun, J. White, *Orthop. Res. Rev.* **2015**, *7*, 107.
[10] T. Patrício, M. Domingos, A. Gloria, P. Bártolo, *Procedia CIRP* **2013**, *5*, 110.
[11] S. C. Ligon, R. Liska, J. Stampfl, M. Gurr, R. Mülhaupt, *Chem. Rev.* **2017**, *117*, 10212.
[12] K. Cheng, P. Mukherjee, I. Curthoys, *Virtual Phys. Prototyp.* **2017**, *12*, 241.
[13] J. M. Chacón, M. A. Caminero, E. García-Plaza, P. J. Núñez, *Mater. Des.* **2017**, *124*, 143.
[14] J. Torres, J. Cotelo, J. Karl, A. P. Gordon, *JOM* **2015**, *67*, 5.
[15] L. Wang, W. M. Gramlich, D. J. Gardner, *Polymer* **2017**, *114*, 242.
[16] A. El-Hadi, R. Schnabel, E. Straube, G. Müller, S. Henning, *Polym. Test.* **2002**, *21*, 665.
[17] J. F. V. Vincent, *Structural Biomaterials*, Princeton University Press, NJ **2012**.
[18] S. Saeidlou, M. A. Huneault, H. Li, C. B. Park, *Prog. Polym. Sci.* **2012**, *37*, 1657.
[19] V. Srinivas, C. S. J. van Hooy-Corstjens, J. A. W. Harings, *Polymer* **2018**, *142*, 348.
[20] L. Wang, D. J. Gardner, *Prog. Addit. Manuf.* **2018**, https://doi.org/10.1007/s40964-018-0041-7.
[21] S. Andjelic, R. C. Scogna, *J. Appl. Polym. Sci.* **2015**, *132*, 1.
[22] M. Ivey, G. W. Melenka, J. P. Carey, C. Ayranci, *Adv. Mfg. Polymer Comp. Sci.* **2017**, *3*, 81.
[23] H. Zhou, T. B. Green, Y. L. Joo, *Polymer* **2006**, *47*, 7497.
[24] T. Huang, M. Yamaguchi, *J. Appl. Polym. Sci.* **2017**, *134*, 44960.
[25] T. Huang, M. Miura, S. Nobukawa, M. Yamaguchi, *Biomacromolecules* **2015**, *16*, 1660.
[26] PN-EN ISO 178:2011 Plastics – Determination of Flexural Properties.
[27] PN-EN ISO 527-2:2012 Preview Plastics – Determination of Tensile Properties, Part 2: Test Conditions for Moulding and Extrusion Plastics.

[28] E. W. Fischer, H. J. Sterzel, G. Wegner, *Kolloid-Zu Z-Polymer* **1973**, *251*, 980.
[29] J. I. Langford, A. J. C. Wilson, *J. Appl. Cryst.* **1978**, *11*, 102.
[30] S. Farah, D. G. Anderson, R. Langer, *Adv. Drug Deliv. Rev.* **2016**, *107*, 367.
[31] M. Yasuniwa, S. Tsubakihara, Y. Sugimoto, C. Nakafuku, *J. Polym. Sci. Part B Polym. Phys.* **2004**, *42*, 25.
[32] H. Tsuji, Y. Ikada, *Macromol. Chem. Phys.* **1996**, *197*, 3483.
[33] O. Wachsen, K. Platkowski, K.-H. Reichert, *Polym. Degrad. Stab.* **1997**, *57*, 87.
[34] G. Perego, G. D. Cella, C. Bastioli, *J. Appl. Polym. Sci.* **1996**, *59*, 37.
[35] F. Carrasco, P. Pagès, J. Gámez-Pérez, O. O. Santana, M. L. Maspoch, *Polym. Degrad. Stab.* **2010**, *95*, 116.
[36] M. Savaris, V. dos Santos, R. N. Brandalise, *Mater. Sci. Eng. C* **2016**, *69*, 661.
[37] J. Jozwiakowska, R. A. Wach, B. Rokita, P. Ulanski, S. P. Nalawade, D. W. Grijpma, J. Feijen, J. M. Rosiak, *Polym. Degrad. Stab.* **2011**, *96*, 1430.
[38] P. Nugroho, H. Mitomo, F. Yoshii, T. Kume, *Polym. Degrad. Stab.* **2001**, *72*, 337.
[39] A. Schindler, D. Harper, *J. Polym. Sci. Polym. Chem.* **1979**, *17*, 2593.

